Mol. Cells *29*, 363-371, April 30, 2010
DOI/10.1007/s10059-010-0045-8

Molecules and Cells

An Archaeal NADH Oxidase Causes Damage to Both Proteins and Nucleic Acids under Oxidative Stress

Baolei Jia[1], Sangmin Lee[1], Bang P. Pham[1], Yoon Seung Cho[1], Jae-Kyung Yang[2], Hee-Seop Byeon[2], Jong Cheol Kim[3], and Gang-Won Cheong[1,4,*]

NADH oxidases (NOXs) catalyze the two-electron reduction of oxygen to H_2O_2 or four-electron reduction of oxygen to H_2O. In this report, we show that an NADH oxidase from *Thermococcus profundus* (NOXtp) displays two forms: a native dimeric protein under physiological conditions and an oxidized hexameric form under oxidative stress. Native NOXtp displays high NADH oxidase activity, and oxidized NOXtp can accelerate the aggregation of partially unfolded proteins. The aggregates formed by NOXtp have characteristics similar to β-amyloid and Lewy bodies in neurodegenerative diseases, including an increase of β-sheet content. Oxidized NOXtp can also bind nucleic acids and cause their degradation by oxidizing NADH to produce H_2O_2. Furthermore, *Escherichia coli* cells expressing NOXtp are less viable than cells not expressing NOXtp after treatment with H_2O_2. As NOXtp shares similar features with eukaryotic cell death isozymes and life may have originated from hyperthermophiles, we suggest that NOXtp may be an ancestor of cell death proteins.

INTRODUCTION

NADH oxidases are widespread in both prokaryotic and eukaryotic cells and have diverse functions. In several bacteria and archaea, NADH oxidases maintain the intracellular redox balance, recycle oxidized pyridine nucleotides, and protect against oxidative stress (Kawasaki et al., 2004; Miyoshi et al., 2003). In eukaryotic cells, NADH oxidases located in the plasma membrane are able to transfer electrons from cytoplasmic NADH to extracellular electron acceptors, thereby maintaining an appropriate intracellular NADH/NAD^+ ratio (Morré and Brightman, 2008). Apoptosis inducing factor (AIF), which can also function as an NADH oxidase, has been well studied in eukaryotes. In healthy cells, AIF is located in mitochondria and is essential for optimal oxidative phosphorylation and antioxidant defense through its NADH oxidase function. Under certain stress conditions, AIF is released from the mitochondria and translocates to the nucleus from the cytosol. In the nucleus, it can cause chromatin condensation and DNA degradation, contributing to cell death (Modjtahedi et al., 2006; Vahsen et al., 2005).

The accumulation of intracellular and extracellular protein aggregates is characteristic of neurodegenerative disorders and the early stages of cell death (Forman et al., 2004; Ross and Poirier, 2006). For instance, Lewy bodies, a feature of Parkinson's disease, are aggregates of α-synuclein, which undergoes conformational changes to acquire a predominantly β-sheet structure in fibrils (Conway et al., 2000). Oxidative stress induces the amyloid-like aggregation of glyceraldehyde-3-phosphate dehydrogenase, a pro-apoptotic protein, which can promote cell death in eukaryotic cells (Nakajima et al., 2007). Programmed cell death in prokaryotes is mediated by toxin-antitoxin modules, but has not been studied as intensively in prokaryotes as in eukaryotes (Engelberg-Kulka et al., 2006; Hayes, 2003). Moreover, the relationship between eukaryotic and prokaryotic cell death is not clear, and no common pathways have been identified for cell death in eukaryotes and prokaryotes (Koonin and Aravind, 2002; Vahsen et al., 2005).

Recently, we isolated an NADH oxidase from *Thermococcus profundus* (NOXtp). NOXtp can use both NADH and NADPH as electron donors to reduce O_2 to H_2O predominantly, which is more favor to detoxify O_2. NOXtp contains a cysteinyl redox center at Cys45 in addition to FAD, and Cys45A mutants produce H_2O_2 (Jia et al., 2008). Here, we demonstrate that NOXtp is a dimer under the physiological conditions of *T. profundus*, but oxidative and cold stresses induce NOXtp oligomerization. Oxidized NOXtp accelerates the aggregation of partially unfolded proteins and binds nucleic acids. We proposed that NOXtp is thus the first archaeal protein to show cell death activity.

MATERIALS AND METHODS

Purification and storage of NOXtp under anaerobic conditions

NOXtp was purified according to a previously described method

[1]Division of Applied Life Sciences (Brain Korea 21 Program), Gyeongsang National University, Jinju 660-701, Korea, [2]Division of Environmental Forest Science, Gyeongsang National University, Jinju 660-701, Korea, [3]Institute of Hadong Green Tea, Hadong 667-882, Korea, [4]Environmental Biotechnology National Core Research Center, Gyeongsang National University, Jinju 660-701, Korea
*Correspondence: gwcheong@gnu.ac.kr

Received December 4, 2009; revised December 18, 2009; accepted December 23, 2009; published online March 4, 2010

Keywords: cell death, dual function, NADH oxidase, protein aggregation, thermophilic archaeon

(Jia et al., 2008) with the following modifications: 50 mM potassium phosphate buffer was equilibrated with purified nitrogen gas in an anaerobic chamber for 24 h to remove O_2, and 0.05% Na_2S was added to remove traces amounts of O_2. This O_2-free buffer was stocked in anaerobic vials and was used in all purification steps and to store a stock solution of the protein. Purified NOXtp could be stored in anaerobic vials for one week at 4°C. The Na_2S was removed with a Centricon centifugal filter (Millipore, USA) before use.

Oxidative stress to NOXtp, native-PAGE, reducing SDS-PAGE, and nonreducing SDS-PAGE

O_2 and H_2O_2 stress were performed as follows: for O_2 stress, NOXtp in O_2-free buffer was dialyzed with air-saturated 50 mM potassium phosphate buffer for 48 h at 4°C. For H_2O_2 stress, NOXtp was treated with 10 mM H_2O_2 at 4°C overnight, and then H_2O_2 was removed by dialysis with O_2-free 50 mM potassium phosphate buffer. For native PAGE, 20 μg of protein with or without oxidative stress was incubated at 37°C or 80°C for 2 h, mixed with loading buffer (80 mM Tris, 10% glycerol, 0.002% bromphenol blue, pH 6.8), and applied to a 7.5% native PAGE gel immediately. For nonreducing SDS-PAGE and reducing SDS-PAGE, 12.5% gels were used; sample buffers contained 2% SDS for nonreducing SDS-PAGE and both 2% SDS and 5% β-mercaptoethanol for reducing SDS-PAGE. After electrophoresis, gels were stained directly with Coomassie brilliant blue.

Electron microscopy

NOXtp (0.05 μg) treated as described above or protein mixtures (0.05 μg) containing NOXtp and lysozyme were absorbed to glow-discharged carbon-coated copper grids by incubation for 2 min, then the grids were rinsed with deionized water and stained with 2% uranyl acetate. The images were recorded with a Philips Tecnai transmission electron microscope (TEM) at an accelerated voltage of 120 kV and a magnification of 52,000-fold. Light-optical diffractograms were used to select micrographs to avoid defocus and to verify that no drift or astigmatism was present. Image processing was performed with the SEMPER and EM software packages (Hegerl, 1996). Particles in a 64 × 64 pixel frame were extracted and aligned translationally and rotationally by correlation methods and finally subjected to multivariate statistical analysis (Kang et al., 2003; Kim et al., 2000; Van Heel and Frank, 1981).

Western blotting

T. profundus cells were cultured at 80°C for about 5 h until OD_{600} = 0.5. For O_2 stress, purified air with a flow rate of 5 L/min was injected into the anaerobic culture bottles for 20 min until a redox indicator (Reazurin, 0.1 mg/L) turned pink. After the O_2 injection, the cells were maintained for 24 h at 80°C. For H_2O_2 treatment, the bottles were injected with H_2O_2 to a final concentration of 100 mM, and the cells were maintained for 24 h at 80°C (Marteinsson et al., 1997). For cold stress, the cells were transferred to a 37°C water bath and were cultured for a further 24 h. Oxidative stresses at low temperature were performed as they were at 80°C. After the stress treatment, cells were dissolved in 50 mM O_2-free potassium phosphate buffer and disrupted by sonication; 40 μg of total soluble protein was applied to native PAGE gels. After electrophoresis, the proteins were transferred to poly(vinylidene difluoride) membranes. The membranes were saturated with 5% nonfat dry milk powder in PBS/0.1% Tween-20 at room temperature for 2 h, followed by incubation with a polyclonal antibody against NOXtp for 3 h. After 3 washes with PBS/0.1% Tween-20, the membranes were incubated with a solution of anti-rabbit Ig conjugated with alkaline phosphatase. After 1-h incubation at room temperature, the membranes were washed and the membrane blots were developed with EZ/ECL reagents. The quantity of protein was determined with 'Quantity One' (BioRad, USA).

Enzyme activity assays

The NADH oxidase activity of NOXtp was examined by time-dependent removal of NADH in the aerobic state. The assay was performed in 50 mM sodium phosphate buffer (pH 7.2), containing 0.5 mM NADH, 1 mM EDTA, and 100 mM NaCl. The reaction was started by adding NOXtp. The rate of NADH consumption was measured by monitoring the decrease in absorbance at 340 nm.

H_2O_2 was detected using a PeroxiDetect Kit (Sigma, USA). Briefly, the assay was performed in 50 mM sodium phosphate buffer (pH 7.2), 100 μmol NAD(P)H, 1 mM EDTA, 100 mM NaCl, and 0.2 nmol NOXtp. The reaction was allowed to finish completely. Reaction buffer (100 μl) was added to the kit. Peroxides convert Fe^{2+} to Fe^{3+} ions under acidic conditions. Fe^{3+} ions will then form a colored adduct with xylenol orange, which can be observed at 560 nm. NAD(P)H will interfere with the H_2O_2 assay, so all of the NAD(P)H must be consumed completely.

To trigger aggregation at low temperature, the heat shock temperature (45°C) of citrate synthase (CS) from porcine heart mitochondria (Sigma) was used (34). Native CS was diluted to a final concentration of 0.2 μM in a pre-warmed buffer (50 mM sodium phosphate, 100 mM NaCl, pH 7.2) with the same molarity of native NOXtp or NOXtp oxidized by H_2O_2 or O_2. Aggregation of proteins was monitored by measuring the time course of the absorbance at 360 nm using a spectrophotometer with an attached thermostatic cell holder assembly maintained at 45°C. The same procedures were performed with hen egg lysozyme at 65°C (Chang and Li, 2002; Klunk et al., 1999) and malate dehydrogenase (MDH; Sigma) from *Thermus aquatics* at 80°C (Hongo et al., 2006).

To measure whether NOXtp affects denatured proteins, hen egg-white lysozyme was dissolved in denaturing buffer (6 M guanidine-HCl, 100 mM NaCl, 20 mM sodium phosphate, 50 mM dithiothreitol, pH 7.2) and then diluted 100× to a final concentration of 0.2 μM in 50 mM sodium phosphate buffer alone or the buffer containing the same molarity of NOXtp. Aggregation of the substrate was monitored spectrophotometrically at 360 nm for 10 min at 25°C (Lundin et al., 2004).

The bactericidal action of lysozyme was measured as follows: the same amount of lysozyme alone or lysozyme treated with NOXtp was mixed with a suspension of *E. coli* (XL1-Blue) cells (10^5 cells/ml) from a logarithmic-phase culture in 50 mM sodium acetate buffer (pH 5.5) and incubated at 37°C for 30 min. The mixtures were centrifuged to remove the lysozyme, and the pellets were diluted serially and plated onto agar plates. All plates were incubated at 37°C overnight. Viable cell numbers were counted and percent survival was determined based on the number of colonies.

Nucleic acids assay

Different states of NOXtp (5 μg) with 2 μl DNA molecular weight ladders (100-bp DNA mass ladder, 500-bp at 100 ng/μl, others at 50 ng/μl) were incubated for 15 min at the indicated temperatures, and a gel retardation assay was carried out in 1% agarose gels (Vahsen et al., 2005). Samples were electrophoresed in Tris-acetate buffer and stained with ethidium bromide (EtBr).

The effect of NOXtp on DNA was examined using purified pBluescript plasmid as substrate. After incubation the plasmid (100 ng) was treated with NOXtp or NADH as indicated for 2 h

at 37°C, and then the protein was denatured by 2% SDS and removed by phenol-chloroform extraction. The plasmid was purified by ethanol precipitation and analyzed by electrophoresis in a 0.8% agarose gel to separate the supercoiled and damaged fractions (Geri et al., 2001).

RNA was purified from *E. coli* by the phenol extraction method (Joseph and Russell, 2001). All buffers in the RNA experiment were treated with diethypyrocarbonate (DEPC) and autoclaved 30 min to denature the DEPC. Like the DNA binding assay, the RNA-NOXtp binding assay was performed using gel retardation in 1.2% agarose gels. The effect of NOXtp (5 μg) on RNA (100 ng) was assayed following the same methods as in the DNA assay except that the RNA was analyzed in a 1.2% agarose gel.

Congo red absorbance assay for aggregates formation

Congo red (20 μM) in 50 mM potassium phosphate buffer (pH 7.4) was prepared and filtered through a 0.2-μm polyether sulfone filter. NOXtp (5 μg) in different states was mixed with lysozyme (10 μg) and incubated at 37°C or 65°C for 10 min. Aliquots of the mixtures (5 μl) were added to 250 μl of 20 μM congo red. After incubation on a rotary shaker at room temperature for 30 min, absorbance data were collected at 540 nm with a spectrophotometer (Conway et al., 2000; Klunk et al., 1999).

Cell culture

E. coli cells of BL21(DE3) containing pNOXtp or pET28(a) were cultured overnight at 37°C in LB broth. A 100-μl sample of this overnight culture was used to inoculate 20 ml LB. Cultures in logarithmic phase (OD_{600} = 0.5) were induced for 3 h with 1.0 mM isopropyl-β-d-thiogalactopyranoside (IPTG) at 37°C. As controls, samples were also continually cultured for 3 h without IPTG at 37°C. Equal amounts of cells were diluted in LB broth containing 50 mg/ml kanamycin (Laksanalamai et al., 2003). Diluted samples (50 μl) were treated with 200 mM H_2O_2 at 37°C for 30 min in shaker. Samples were diluted 10 × with LB broth, centrifuged, and resuspended with 50 μl LB broth to remove the H_2O_2. The resuspended cells were diluted and plated on LB agar containing kanamycin, and the plates were incubated at 37°C overnight. Cell viability was determined after overnight incubation.

RESULTS

Conformational change of NOXtp induced by stress

Previously, we showed that NOXtp forms a hexameric ring-shaped assembly (50 kDa × 6) at room temperature under reducing and aerobic conditions (Jia et al., 2008), but its thermophilic and mesophilic homologs, such as NADH oxidase from *Thermus thermophilus* and *Lactobacillus sanfranciscensis*, are generally dimeric (Hecht et al., 1995; Lountos et al., 2006). We examined whether NOXtp, which is from an anaerobic thermophilic organism, assumes different structures under different conditions. In a native polyacrylamide gel electrophoresis (PAGE) analysis (Fig. 1A) the molecular weight (MW) of NOXtp at 80°C in anaerobic conditions was between 67 and 144 kDa, indicating that, like its homologs, it can exist as a dimer. Under oxidative conditions (in the presence of O_2 or H_2O_2), most of the proteins had a MW of 300 kDa. However, NOXtp under cold stress (37°C) displayed 3 bands in anaerobic buffer: the largest hexamer form, the smallest dimer form, and a middle form that appeared to be intermediate between the dimer and hexamer. In aerobic buffer, NOXtp had a MW of 300 kDa at 37°C, consistent with our previous result. Unlike the result from native PAGE, reducing sodium dodecyl sulfate (SDS)-PAGE revealed a single band with a MW of 50 kDa, which is the monomeric size.

In order to further verify the native PAGE result, we examined NOXtp folding by using transmission electron microscopy (TEM). Under physiological conditions (80°C and anaerobic), NOXtp did not display any hexameric forms in the electron micrograph (Fig. 1Ba), whereas O_2- and H_2O_2-oxidized proteins showed hexameric forms (Figs. 1Bb and 1Bc), in accordance with the native PAGE results. At low temperature (37°C) and in anaerobic conditions, NOXtp showed heterogeneous forms (Fig. 1Bd), similar to the 3 bands seen in native PAGE. NOXtp oxidized by O_2 and H_2O_2 was hexameric at 37°C (Figs. 1Be and 1Bf), equivalent to the 300-kDa proteins in native PAGE. We subjected the two most homogeneous samples (native and H_2O_2-treated) to image processing at physiological temperature (80°C) to ascertain the folding states. A total of 308 particles observed in anaerobic buffer at 80°C were translationally aligned and subjected to multivariate statistical analysis. The unsymmetrized average image (Fig. 1Ca) revealed an unequivocal 2-fold symmetry with broad, high accumulation near the ends and tapering towards the middle. The length and width of the 2-fold structure were 13 nm and 7 nm, respectively. The unsymmetrized image of oxidized NOXtp (Fig. 1Cb) showed a hexameric form with diameters of outer ring, 19 nm; middle ring, 15 nm; and cavity, 4 nm. Collectively, the results of the native PAGE, TEM, and image processing indicate that NOXtp exists as dimer under native conditions, and the dimers assemble into hexamers under stress. H_2O_2 was the strongest stressor, followed by O_2 and cold stress.

To confirm the *in vitro* results, we used native PAGE and Western blotting to probe NOXtp assembly *in vivo*. NOXtp obtained from normal *T. profundus* cells existed in a dimeric form (Fig. 1D), similar to the recombinant protein shown in Fig. 1A. Under cold stress, NOXtp displayed 2 forms: dimer and hexamer. There was no intermediate form as there had been with the recombinant protein from *E. coli*, perhaps because some *in vivo* factors stabilize NOXtp. When the cells were subjected to oxidative stress, NOXtp was in the hexameric form. NOXtp expression increased substantially under different stresses. The relative expression determined from the Western blotting film density (Fig. 1D) showed an increase of about 2-fold under cold stress, a 5- to 6-fold increase under O_2 and H_2O_2 stress at physiological temperature, and a 3- to 4-fold increase under O_2 and H_2O_2 stress at low temperature. This result suggests that NOXtp, a flavoprotein that can reduce O_2 by oxidizing NADH or NADPH, plays an important role in oxidative stress. The consistent results from the *in vitro* and *in vivo* analyses indicate that NOXtp switches from a low-MW dimer under normal conditions to a high-MW oligomer in the presence of oxidative and cold stresses.

Conformational change of NOXtp accompanies a functional switch

We next assayed enzyme activities to study the function of the two different structural forms of NOXtp. Both H_2O_2 and O_2 treatment caused NOXtp to lose its NADH oxidase activity at 37°C and 80°C (Figs. 2Aa and 2Ab). The product of NOXtp also switched from H_2O to H_2O_2 (Fig. 2Ac), suggesting that the active site at Cys45 was partially oxidized to R-SO_2H or R-SO_3H (Ward et al., 2001). Some proteins with oligomeric structure or that switch to oligomeric forms in response to stress either show chaperone activity to prevent protein aggregation (Chuang et al., 2006; Jang et al., 2001; Kim et al., 2006; Lee et al., 2009) or actually form aggregates, therefore promoting

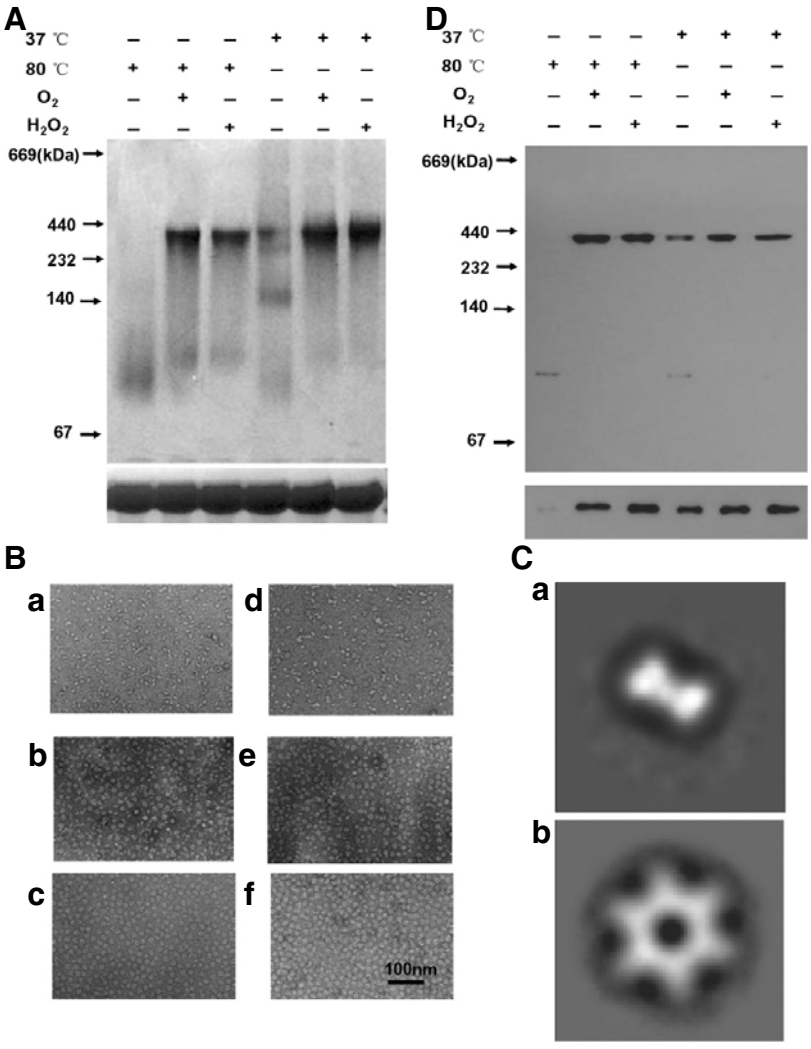

Fig. 1. Conformational changes of NOXtp induced by stress. (A) Native PAGE (7.5%) of NOXtp under different conditions. A stock solution of purified NOXtp in O_2-free buffer was treated as described in the "Materials and Methods". The different conditions are shown at the top of the gel. MW markers (kDa) are shown to the left. The lower part shows the same proteins in reducing SDS-PAGE. (B) Electron micrographs of NOXtp under different conditions. The scale bar represents 100 nm. The samples in (a), (b), and (c) were incubated at 80°C and those in (d), (e), and (f) were incubated at 37°C. (a) and (d), NOXtp in O_2-free buffer; (b) and (e), treated with O_2; (c) and (f), treated with H_2O_2. (C) multivariate statistical analysis of NOXtp. In (a), unsymmetrized averages of native NOXtp were derived from 308 translationally aligned particles of NOXtp at 80°C in anaerobic buffer. In b, the average of 211 end-on views of NOXtp at 80°C treated with H_2O_2. (D) NOXtp expression in response to different stresses. Equal amounts of crude proteins extracted from *T. profundus* under different stress conditions were separated by 7.5% native PAGE and subjected to immunoblotting with an anti-NOXtp polyclonal antibody. The different stresses and temperatures are shown at the top of the gel. The lower part shows the same proteins separated by reducing SDS-PAGE and detected by the anti-NOXtp polyclonal antibody.

apoptotic activity (Nakajima et al., 2007). We used two model proteins, citrate synthase (CS) from porcine heart mitochondria and malate dehydrogenase (MDH) from *Thermus aquatics*, as substrates to determine the effects of NOXtp on other macromolecules. In the assay, aggregation is triggered by incubation at high temperatures, and the extent of aggregation is measured by light absorbance. During incubation at 45°C, thermal aggregation of CS was observed (Fig. 2Ba). Aggregation was promoted in the presence of oxidized NOXtp, and native NOXtp had no substantial effect on aggregation. Similar results were obtained during incubation with MDH at 80°C (Hongo et al., 2006), a temperature at which MDH will aggregate (Fig. 2Bb). Moreover, oxidized NOXtp efficiently accelerated the aggregation of reduced and denatured lysozyme (Fig. 2C). Thus, oxidative stresses not only decrease the NADH oxidase activity of NOXtp, but also increase its contribution to the formation of aggregates of abnormal proteins.

Mechanism of oxidized NOXtp-induced protein aggregation

To further determine how NOXtp promotes protein aggregation, we used lysozyme as a substrate. Lysozyme is a model protein for studying protein folding and is partially denatured at 65°C (Chang and Li, 2004; Colombié et al., 2001; Goldberg et al., 1991). Lysozyme heated to 65°C in the presence of oxidized NOXtp showed much higher absorbance at 360 nm than in the presence of native NOXtp (Supplementary Fig. 1A), implying that lysozyme was more extensively aggregated in the presence of oxidized NOXtp than of native NOXtp. We further examined the aggregates with EM (Fig. 3A), which showed that lysozyme formed much larger aggregates with oxidized NOXtp than with native or no NOXtp. Furthermore, lysozyme aggregates formed with oxidized NOXtp at 65°C could be precipitated by centrifugation, and the aggregates contained both proteins (Supplementary Fig. 1B). In contrast, lysozyme with native NOXtp, lysozyme alone at high temperature, and lysozyme with NOXtp at low temperature did not form big aggregates that could be precipitated. These results show that only oxidized NOXtp and a partially unfolded protein can form big aggregates composed of both proteins (Supplementary Fig. 1B).

Native lysozyme contains 4 pairs of cysteines that form disulfide bridges within the molecule. Thermoinactivation of lysozyme at neutral pH is accompanied by intra- and intermolecular disulfide exchange (Chang and Li, 2004). Nonreducing SDS-PAGE (Fig. 3B) showed that lysozyme did not form intermolecular disulfide bonds at 37°C in the presence or absence of any NOXtp. After heating to 65°C, a trace amount of dimerized lysozyme appeared in the presence of lysozyme alone or lysozyme with native NOXtp. High-MW lysozyme did form in the presence of

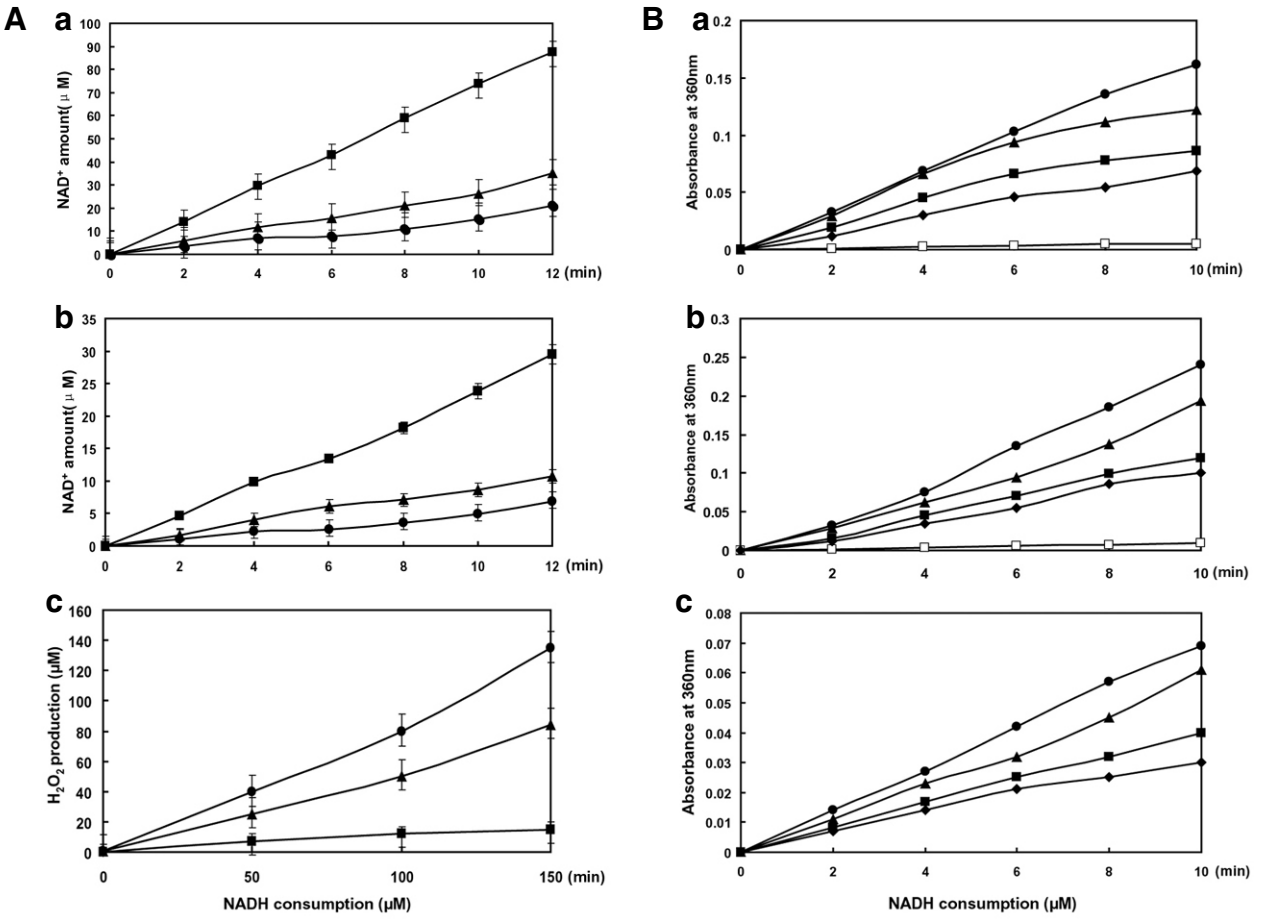

Fig. 2. Effects of NOXtp state on NADH oxidase activity and thermal aggregation of citrate synthase (CS) and malate dehydrogenase (MDH). (A) Time course of effect of stress on NADH oxidase activity. NADH oxidase activity of native NOXtp (■), O_2-oxidized NOXtp (▲), and H_2O_2-oxidized NOXtp (●) was measured at 80°C (a) and 37°C (b) in the presence of 20 nM NOXtp and 0.5 mM NADH. (c) The amount of H_2O_2 produced by native NOXtp (■), O_2-oxidized NOXtp (▲), and H_2O_2-oxidized NOXtp (●) when 100 μM NADH were oxidized. (B) Thermal aggregation of CS at 45°C (a) and MDH at 80°C (b). Aggregation of the substrates was induced at the indicated temperatures in solutions containing 0.2 μM substrate alone (◆), substrate with the same molar concentration of native NOXtp (■), O_2 oxidized NOXtp (▲), and H_2O_2-oxidized NOXtp (●). H_2O_2-oxidized NOXtp alone (□), without substrate, was used as a control. (C) NOXtp induces aggregation of denatured lysozyme. Relative aggregation of 0.2 μM denatured lysozyme in buffer alone (◆) or in the presence of the same molar of native NOXtp (■), O_2-oxidized NOXtp (▲), and H_2O_2-oxidized NOXtp (●).

oxidized NOXtp at 65°C, and the high-MW protein could be disrupted by β-mercaptoethanol, indicating it was formed by disulfide bonds (Fig. 3B). Thus, the aggregates formed by NOXtp are due to incorrect disulfide bond formation, which will lead to improper protein folding.

Aggregates causing neurodegenerative diseases and apoptosis usually consist of fibers containing misfolded proteins with β-sheet stacking (Conway et al., 2000; Forman et al., 2004). Congo red is a histologic dye that binds many aggregated proteins because of their extensive β-sheet structure, and this binding leads to increased absorbance at 540 nm (Klunk et al., 1999). A Congo red assay (Fig. 3C) showed that heating lysozyme to 65°C increased the amount of β-sheets substantialy more in the presence of oxidized NOXtp than in the presence of native NOXtp. NOXtp in any state had no effect on the relative amount of β-sheets at low temperature.

Finally, bactericidal assays (Fig. 3D) showed that NOXtp in any state can not effect *E. coli* survivals (data not shown) and NOXtp had no effect on the activity of lysozyme at low temperature, but oxidized NOXtp decreased its activity substantially at 65°C. This result indicated that protein aggregation inactivated lysozyme function.

Oxidized NOXtp damages DNA and RNA

Because AIF in eukaryotes both acts as an NAD(P)H oxidase and induces apoptosis by DNA condensation (Modjtahedi et al., 2004; Vahsen et al., 2005), we hypothesized that NOXtp can also bind DNA and RNA. Native NOXtp did not cause significant DNA retention in horizontal gel electrophoresis at low or high temperatures, but H_2O_2- and O_2-oxidized NOXtp reduced the electrophoretic mobility of DNA (Fig. 4Aa). A vertical gel retardation assay confirmed that oxidized NOXtp can bind DNA (Supplementary Fig. 2A). Similarly, oxidized NOXtp bound total RNA from *E. coli* tightly, preventing it from entering the gel in a dose-dependent manner, but native NOXtp did not clearly prevent RNA mobility in an agarose gel (Fig. 4Ab). Bovine serum albumin had no effect on RNA mobility, further confirming that oxidized NOXtp can bind RNA (Supplementary Fig. 2B).

NOXtp in any state showed no DNase or RNase activity (Figs. 4Ba and 4Bc). However, in the presence of NADH, su-

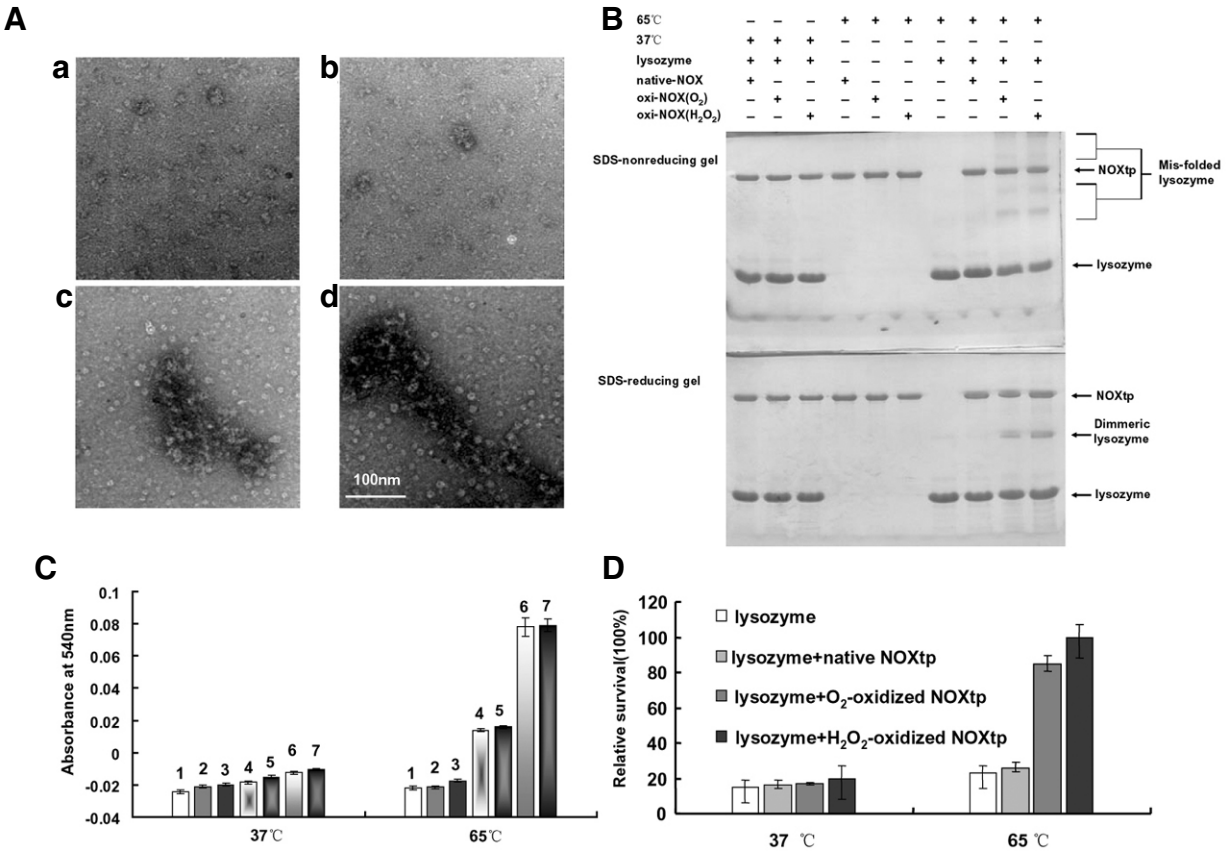

Fig. 3. Characteristics of lysozyme aggregates caused by NOXtp. (A) Electron micrographs of lysozyme alone (a) and lysozyme with native NOXtp (b), O_2-oxidized NOXtp (c), and H_2O_2-oxidized NOXtp (d) after incubation at 65°C for 10 min. (B, C) Aggregate formation caused by NOXtp was accompanied by inappropriate disulfide bonds and β-sheet accumulation. (B) NOXtp in different states was incubated with lysozyme at 37°C or 65°C for 10 min. The misfolded lysozyme was analyzed with reducing and nonreducing SDS-PAGE. (C) Congo red binding assay to analyze the relative amount of β-sheets in aggregates. Bars 1, 2, 3, 4, 5, 6, and 7 indicate the relative β-sheet content of native NOXtp, O_2-oxidized NOXtp, H_2O_2-oxidized NOXtp, lysozyme, lysozyme with native NOXtp, lysozyme with O_2-oxidized NOXtp, and lysozyme with H_2O_2-oxidized NOXtp at 37°C (left) and 65°C (right). (D) Effect of NOXtp on the bactericidal action of lysozyme. Lysozyme alone or lysozyme with different forms of NOXtp were treated at 37°C (left) and 65°C (right) and then *E. coli* cells were incubated with these proteins. The relative survival of *E. coli* was calculated based on the number of cells on the plates.

percoiled plasmid DNA was damaged by the introduction of single-stranded or double-stranded breaks that could be seen by changes in mobility through the agarose gel (Figs. 4Ba and 4Bb). Similarly, total RNA was also degraded by oxidized NOXtp with NADH (Figs. 4Bc and 4Bd). Native NOXtp had no effect on the stability of DNA and RNA. Damage to nucleic acids by NOXtp in the presence of NADH increased considerably with increasing amounts of NADH, but the damage could be prevented in buffer lacking O_2, even with a large amount of NADH (Figs. 4Bb and 4Bd). These results indicate that the damage to nucleic acids depends on the production of H_2O_2 by the NADH oxidase activity of oxidized NOXtp (Fig. 2Ac), and native NOXtp, which produces H_2O, will not cause degradation.

Survivability of H_2O_2-treated *E. coli* in the presence of NOXtp

Because no convenient system is currently available to study the genetics of archaea, we utilized *E. coli* to examine the biological roles of archaea proteins (Laksanalamai et al., 2003). The BL21 (DE3) strain was transformed with pET28(a) or pNOXtp, which expresses NOXtp when induced by isopropyl-β-d-thiogalactopyranoside (IPTG). In normal growth conditions, the 4 samples (*E. coli* containing pET, induced or not induced by IPTG, and *E. coli* containing pNOXtp, induced or not induced by IPTG) had similar growth rates, as determined by measuring OD_{600}. The recombinant NOXtp, which showed diverse oligomeric forms determined by Western blotting, could only be expressed in the presence of both pNOXtp and IPTG in *E. coli* (Fig. 5A). But after the same amounts of cells were treated with H_2O_2, recombinant NOXtp only existed as hexameric forms and *E. coli* expressing NOXtp was less viable than the other samples (Fig. 5B). This result suggests that expression of NOXtp accelerates the oxidatively induced cell death of *E. coli*.

DISCUSSION

The function of a protein relies on the structure and multifunctional protein always employs different conformations at the active site, shape and size to enable it to fit the intended substrates. NOXtp adopts two conformations including native dimeric form at physiological conditions and oxidized hexameric form at stress conditions. The stress induced conformational change implicated that function switch of NOXtp. We proved that the NAD(P)H oxidase activity of NOXtp was suppressed under oxi-

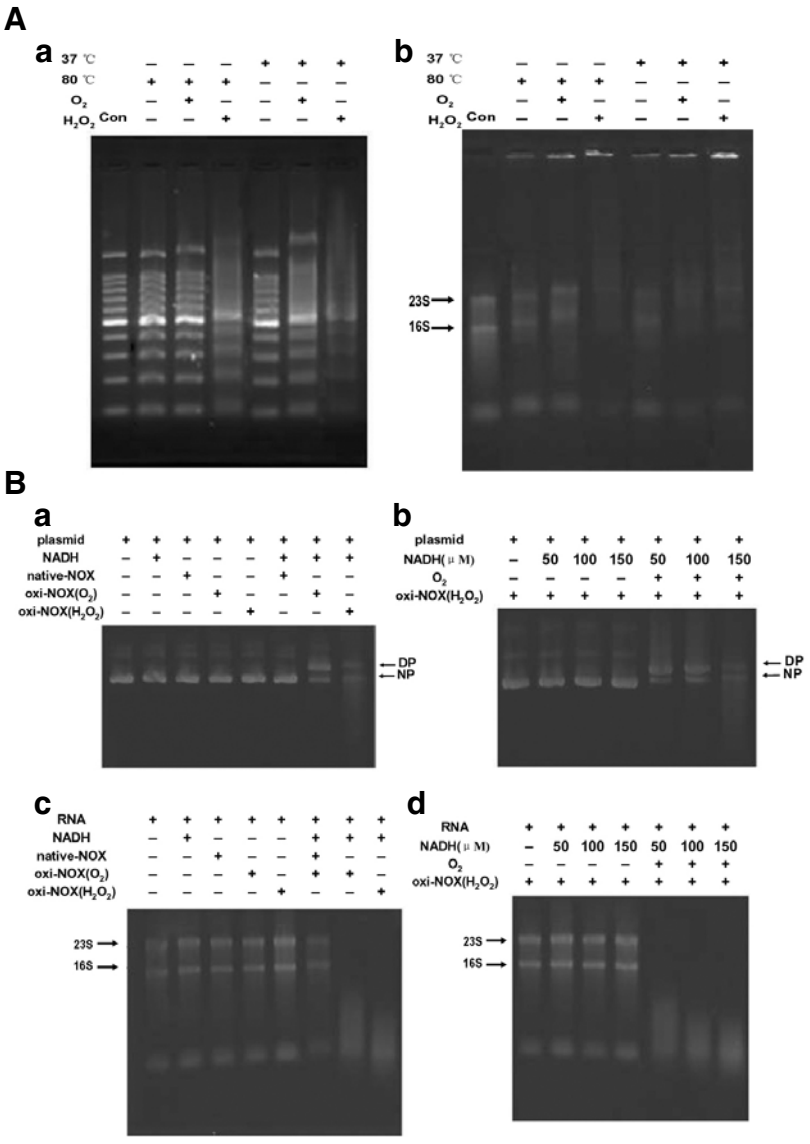

Fig. 4. Interaction of NOXtp with nucleic acids and its effect on nucleic acids. (A) DNA (a) and RNA (b) bind different states of NOXtp. (a) NOXtp was mixed with a DNA marker at the indicated temperature for 15 min; then the DNA was separated by agarose gel electrophoresis and visualized with EtBr. (b) The experiment was carried out as in (a), with the difference that DNA was replaced by total RNA from *E. coli*. (B) NOXtp affects the stability of DNA (a and b) and RNA (c and d). NOXtp was incubated with pBluescript plasmid (a) and RNA (c) with or without NADH; then proteins were removed and nucleic acids were resolved by agarose gel electrophoresis. In (b) and (d), pBluescript plasmid (b) and RNA (d) were incubated with H_2O_2-oxidized NOXtp with increasing amounts of NADH in the absence or presence of O_2, and nucleic acids were analyzed as in a and c. 'NP' indicates the native (supercoiled) plasmid and 'DP' indicates the damaged (circular or linear) plasmid. In c, the positions of 23S and 16S RNA are noted.

dative stress and the oxidized NOXtp can initialize protein aggregation of partially misfolded proteins including thermo-inactived CS, MDH, lysozyme and Gnd-HCl denatured lysozyme. Herein we propose a mechanism underlying the structural and functional changes of NOXtp under oxidative or cold stress. When *T. profundus* is exposed to a low amount of O_2, the dimeric form of NOXtp will be upregulated and react with NAD(P)H to detoxify O_2. However, under oxidative stress conditions, some or all of the upregulated NOXtp will be converted to the hexameric protein to speed protein aggregation. Oxidized hexameric NOXtp can bind nucleic acids and produce H_2O_2 to destroy DNA and RNA with the ultimate function of decreasing cell viability.

When the cells are confronted to chemical or physical stress, they can activate the suicidal biochemical machinery leading to apoptotic demise, or activate the defense mechanisms. The choice between the two responses is determined by the intensity of stress, as well as cell-intrinsic parameters (Céline et al., 2004). For instance, oxidative stress and heat shock exposure of yeasts causes the protein structures of peroxiredoxins (Prxs) to shift from low MW species to high MW complexes, with the function switching from peroxidase to chaperone to prevent protein aggregation and inactivation because proteins under stresses render to unfold or misfold by exposing hydrophobic segments (Jang et al., 2004). These hydrophobic segments exposed proteins may yield protein aggregates also, as the exposed hydrophobic residues often lead to aggregation (Goldberg et al., 1991). The aggregates formation was observed a high correlation with cell death, though the mechanism between them is not clear (Ross and Poirier, 2004). Oxidized NOXtp could both accelerate protein aggregation and decrease *E. coli* survivability. We propose that the aggregate formation induced by NOXtp is the choice for cells to perform suicide pathway, in a contrary manner of chaperones to assist cell survival. In prokaryote, cells performing suicide will donate their nutrients to their neighbors instead of draining resources to repair themselves and contribute to the survival of the complex community of prokaryotes.

The aggregates formed by NOXtp with the stacking of β-sheet secondary structure have the same feature with the protein aggregates in eukaryotic cell aging and apoptosis (Conway et al., 2000; Ross and Poirier, 2004). Furthermore, NOXtp can both detoxify O_2 and cause damage to nucleic acids, which are similar to eukaryotic AIF with the vital function of preventing

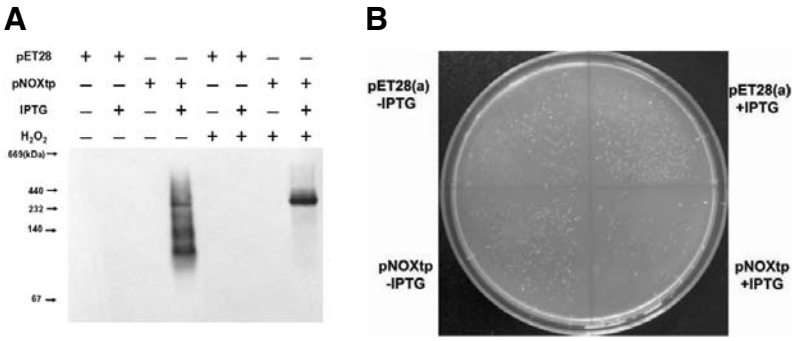

Fig. 5. Host bacteria expressing NOXtp are more sensitive to H_2O_2. *E. coli* cells were transformed with pET28(a) or pNOXtp and expression in the cells was or was not induced by IPTG as indicated. IPTG was removed and equal amounts of cells were treated with H_2O_2, and then the same amount of total proteins from these cells was analyzed by Western blotting with an anti-NOXtp polyclonal antibody (A). Meanwhile, the same cells were diluted and the culture was continued on plates until the cells formed colonies (B).

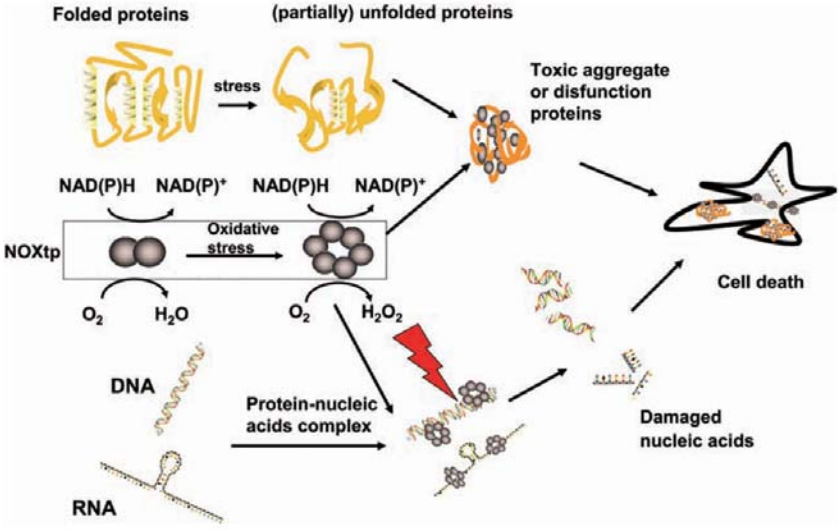

Fig. 6. Schematic presentation of the effect of NOXtp on macromolecules.

oxidative stress through their NAD(P)H oxidase activity and the lethal function of accelerating cell death by causing DNA degradation (Modjtahedi et al., 2006). As the function of NOXtp is similar to eukaryotic cell death proteins and the universal ancestor may be a (hyper) thermophile (Di Giulio, 2001), we propose that NOXtp may be an ancestral protein of the eukaryotic cell death machinery.

Note: Supplementary information is available on the Molecules and Cells website (www.molcells.org).

ACKNOWLEDGMENTS

B. Jia, S. Lee, and B.P. Pham were supported by scholarships from the Brain Korea21 project in 2008, Korea. This work was supported by a grant from the Ministry of Science and Technology/Korea Science and Engineering Foundation to the Environmental Biotechnology National Core Research Center (Grant No. R15-2003-012-01003-0), and the Korea Research Foundation Grant funded by the Korean Government (Ministry of Education and Human Resources Development) (Grant No. KRF-2008-521-C00219), to G.W. Cheong.

REFERENCES

Céline, C., Nicola, V., Didier, M., Hélène, T., Karim, C., Carmen, G., Jamal, T., and Guido, K. (2004). Regulation of cytoplasmic stress granules by apoptosis-inducing factor. J. Cell Sci. *117*, 4461-4468.

Chang, J.Y., and Li, L. (2002). The unfolding mechanism and the disulfide structures of denatured lysozyme. FEBS Lett. *511*, 73-78.

Chuang, M.H., Wu, M.S., Lo, W.L., Lin, J.T., Wong, C.H., and Chiou, S.H. (2006). The antioxidant protein alkylhydroperoxide reductase of *Helicobacter pylori* switches from a peroxide reductase to a molecular chaperone function. Proc. Natl. Acad. Sci. USA *103*, 2552-2557.

Colombié, S., Gaunand, A., and Lindet, B. (2001). Lysozyme inactivation under mechanical stirring: effect of physical and molecular interfaces. Enzyme Microb. Technol. *28*, 820-826.

Conway, K.A., Lee, S.J., Rochet, J.C., Ding, T.T., Williamson, R.E., and Lansbury, P.T. Jr. (2000). Acceleration of oligomerization, not fibrillization, is a shared property of both alpha -synuclein mutations linked to early-onset Parkinson's disease. Proc. Natl. Acad. Sci. USA *97*, 571-576.

Di Giulio, M. (2001). The universal ancestor was a thermophile or a hyperthermophile. Gene *281*, 11-17.

Engelberg-Kulka, H., Amitai, S., Kolodkin-Gal, I., and Hazan, R. (2006). Bacterial programmed cell death and multicellular behavior in bacteria. PLoS Genet. *2*, e135.

Ferreira, R.M., de Andrade, L.R., Dutra, M.B., de Souza, M.F., Flosi Paschoalin, V.M., and Silva, J.T. (2006). Purification and characterization of the chaperone-like Hsp26 from *Saccharomyces cerevisiae*. Protein Expr. Purif. *47*, 384-392.

Forman, M.S., Trojanowski, J.Q., and Lee, V.M. (2004). Neurodegenerative diseases: a decade of discoveries paves the way for therapeutic breakthroughs. Nat. Med. *10*, 1055-1063.

Geri, F.M., Lotta, H., and Nora, G. (2001). Clue to damage recognition by UvrB: .residues in the -hairpin structure prevent binding to non-damaged DNA. EMBO J. *20*, 6140-6149.

Goldberg, M.E., Rudolph, R., and Jaenicke, R. (1991). A kinetic study of the competition between renaturation and aggregation during the refolding of denatured-reduced egg white lysozyme. Biochemistry *30*, 2790-2797.

Hayes, F. (2003). Toxins-antitoxins: plasmid maintenance, programmed cell death, and cell cycle arrest. Science *301*, 1496-

1499.
Hecht, H.J., Erdmann, H., Park, H.J., Sprinzl, M., and Schmid, R.D. (1995). Crystal structure of NADH oxidase from *Thermus thermophilus*. Nat. Struct. Biol. *2*, 1109-1114.
Hegerl, R. (1996). The EM program package: A platform for image processing in biological electron microscopy. J. Struct. Biol. *116*, 30-34.
Hongo, K., Hirai, H., Uemura, C., Ono, S., Tsunemi, J., Higurashi, T., Mizobata, T., and Kawata, Y. (2006). A novel ATP/ADP hydrolysis activity of hyperthermostable group II chaperonin in the presence of cobalt or manganese ion. FEBS Lett. *580*, 34-40.
Jang, H.H., Lee, K.O., Chi, Y.H., Jung, B.G., Park, S.K., Park, J.H, Lee, J.R., Lee, S.S., Moon, J.C., Yun, J.W., et al. (2004). Two enzymes in one: two yeast peroxiredoxins display oxidative stress-dependent switching from a peroxidase to a molecular chaperone function. Cell *117*, 625-635.
Jia, B., Park, S.C., Lee, S.M., Pham, B.P., Yu, R., Le, T.L., Han, S.W., Yang, J.K., Choi, M.S., Baumeister, W., et al. (2008). Hexameric ring structure of a thermophilic archaeon NADH oxidase that produces predominantly H_2O. FEBS J. *275*, 5355-5366.
Joseph, S., and Russell, D.W. (2001). Molecular Cloning: A Laboratory Manual, 3rd ed., (Cold Spring Harbor, NY, USA: Cold Spring Harbor Laboratory).
Kang, M.S., Kim, S.R., Kwack, P., Lim, B.K., Ahn, S.W., Rho, Y.M., Seong, I.S., Park, S.C., Eom, S.H., Cheong, G.W., et al. (2003). Molecular architecture of the ATP-dependent CodWX protease having an N-terminal serine active site. EMBO J. *22*, 2893-2902.
Kawasaki, S., Ishikura, J., Chiba, D., Nishino, T., and Niimura, Y. (2004). Purification and characterization of an H_2O-forming NADH oxidase from *Clostridium aminovalericum*. Arch. Microbiol. *181*, 324-330.
Kim, K.I., Cheong, G.W., Park, S.C., Ha, J.S., Woo, K.M., Choi, S.J., and Chung, C.H. (2000). Heptameric ring structure of the heat-shock protein ClpB, a protein-activated ATPase in *Escherichia coli*. J. Mol. Biol. *303*, 655-666.
Kim, R., Lai, L., Lee, H.H., Cheong, G.W., Kim, K.K., Wu, Z., Yokota, H., Marqusee, S., and Kim, S.H. (2003). On the mechanism of chaperone activity of the small heat-shock protein of *Methanococcus jannaschii*. Proc. Natl. Acad. Sci. USA *100*, 8151-8155.
Klunk, W.E., Jacob, R.F., and Mason, R.P. (1999). Quantifying amyloid beta-peptide (Abeta) aggregation using the Congo red-Abeta (CR-abeta) spectrophotometric assay. Anal. Biochem. *266*, 66-76.
Koonin, E.V., and Aravind, L. (2002). Origin and evolution of eukaryotic apoptosis: the bacterial connection. Cell Death Differ. *9*, 394-404.
Kumar, M.S., Reddy, P.Y., Kumar, P.A., Surolia, I., and Reddy, G.B. (2004). Effect of dicarbonyl-induced browning on alpha-crystallin chaperone-like activity: physiological significance and caveats of *in vitro* aggregation assays. Biochem. J. *379*, 273-282.
Laksanalamai, P., Jiemjit, A., Bu, Z., Maeder, D., and Robb, F. (2003). Multi-subunit assembly of the *Pyrococcus furiosus* small heat shock protein is essential for cellular protection at high temperature. Extremophiles *7*, 79-83.
Lee, J.R., Lee, S.S., Jang, H.H., Lee, Y.M., Park, J.H., Park, S.C., Moon, J.C., Park, S.K., Kim, S.Y., Lee, S.Y., et al. (2009). Heat-shock dependent oligomeric status alters the function of a plant-specific thioredoxin-like protein, AtTDX. Proc. Natl. Acad. Sci. USA *106*, 5978-5983
Lountos, G.T., Jiang, R., Wellborn, W.B., Thaler, T.L., Bommarius, A.S., and Orville, A.M. (2006). The crystal structure of NAD(P)H oxidase from *Lactobacillus sanfranciscensis*. Biochemistry *45*, 9648-9659.
Lundin, V.F., Stirling, P.C., Gomez-Reino, J., Mwenifumbo, J.C., Obst, J.M., Valpuesta, J.M., and Leroux, M.R. (2004). Molecular clamp mechanism of substrate binding by hydrophobic coiled-coil residues of the archaeal chaperone prefoldin. Proc. Natl. Acad. Sci. USA *101*, 4367-4372.
Marteinsson, V.T., Moulin, P., Birrien, J., Gambacorta, A., Vernet, M., and Prieur, D. (1997). Physiological responses to stress conditions and barophilic behavior of the hyperthermophilic vent archaeon *Pyrococcus abyssi*. Appl. Environ. Microbiol. *63*, 1230-1236.
Miyoshi, A., Rochat, T., Gratadoux, J., Le, L.Y., Oliveira, S., and Azevedo, V. (2003). Oxidative stress in *Lactococcus lactis*. Genet. Mol. Res. *2*, 348-358.
Modjtahedi, N., Giordanetto, F., Madeo, F., and Kroemer, G. (2006). Apoptosis-inducing factor: vital and lethal. Trends Cell Biol. *16*, 264-272.
Morré, D., and Brightman, A.O. (2008). NADH oxidase of plasma membranes. J. Bioenerg. Biomembr. *23*, 469-489.
Nakajima, H., Amano, W., Fujita, A., Fukuhara, A., Azuma, Y.T., Hata, F., Inui, T., and Takeuchi, T. (2007). The active site cysteine of the proapoptotic protein glyceraldehyde-3-phosphate dehydrogenase is essential in oxidative stress-induced aggregation and cell death. J. Biol. Chem. *282*, 26562-26574.
Ross, C.A., and Poirier, M.A. (2004). Protein aggregation and neurodegenerative disease. Nat. Med. *10*, S10-17.
Vahsen, N., Cande, C., Dupaigne, P., Giordanetto, F., Kroemer, R.T., Herker, E., Scholz, S., Modjtahedi, N., Madeo, F., Le Cam, E., et al. (2005). Physical interaction of apoptosis-inducing factor with DNA and RNA. Oncogene *25*, 1763-1774.
Van Heel, M., and Frank, J. (1981). Use of multivariate statistics in analysing the images of biological macromolecules. Ultramicroscopy *6*, 187-194.
Ward, D.E., Donnelly, C.J., Mullendore, M.E., van der Oost, J., de Vos, W.M., and Crane, E.J. 3rd. (2001). The NADH oxidase from *Pyrococcus furiosus*. Eur. J. Biochem. *268*, 5816-5823.